Shuttleworth VG, Gaughan L, Nawafa L, Mooney CA, Cobb SL, Sheerin NS, Logan IR. The methyltransferase SET9 regulates TGFB1 activation of renal fibroblasts via interaction with SMAD3. *Journal of Cell Science* 2018, **131**, jcs207761.

© 2018. Published by The Company of Biologists Ltd | Journal of Cell Science (2018) 131, jcs207761. doi:10.1242/jcs.207761

RESEARCH ARTICLE

The methyltransferase SET9 regulates TGFB1 activation of renal fibroblasts via interaction with SMAD3

Victoria G. Shuttleworth[1], Luke Gaughan[2], Lotfia Nawafa[1], Caitlin A. Mooney[3], Steven L. Cobb[3], Neil S. Sheerin[1,*] and Ian R. Logan[1,*,‡]

ABSTRACT

Chronic kidney disease (CKD) is a global socioeconomic problem. It is characterised by the presence of differentiated myofibroblasts, which cause tissue fibrosis in response to TGFB1, leading to renal failure. Here, we define a novel interaction between the SET9 lysine methyltransferase (also known as SETD7) and SMAD3, the principal mediator of TGFB1 signalling in myofibroblasts. We show that SET9-deficient fibroblasts exhibit globally altered gene expression profiles in response to TGFB1, whilst overexpression of SET9 enhances SMAD3 transcriptional activity. We also show that SET9 facilitates nuclear import of SMAD3 and controls SMAD3 protein degradation via ubiquitylation. On a cellular level, we demonstrate that SET9 is broadly required for the effects of TGFB1 in diseased primary renal fibroblasts; SET9 promotes fibroblast migration into wounds, expression of extracellular matrix proteins, collagen contractility and myofibroblast differentiation. Finally, we demonstrate that SET9 is recruited to the α-smooth muscle actin gene in response to TGFB1, providing a mechanism by which SET9 regulates myofibroblast contractility and differentiation. Together with previous studies, we make the case for SET9 inhibition in the treatment of progressive CKD.

KEY WORDS: TGFB1, Fibroblast, Transcriptional regulation, Chronic kidney disease

INTRODUCTION

The earliest histological feature of chronic kidney disease (CKD) is the aberrant accumulation of activated myofibroblasts, the cell type responsible for replacement of normal kidney tissue with fibrosis (Meran and Steadman, 2011). TGFB1 stimulates myofibroblast migration to the site of tissue injury and is a key driver of myofibroblast differentiation, characterised by their expression of α-smooth muscle actin (α-SMA; also known as ACTA2) (Bottinger and Bitzer, 2002; Massagué, 2012). Upon TGFB1 stimulation, α-SMA is incorporated into intracellular stress fibres, conferring contractile properties upon the myofibroblast (Hinz et al., 2001). TGFB1 also stimulates fibrillar collagen-rich extracellular matrix (ECM) production from the myofibroblast (Wynn and Ramalingam, 2012; Zeisberg and Kalluri, 2013). Stress fibres containing α-SMA indirectly transmit mechanical tension through this ECM, maintaining myofibroblast differentiation and facilitating tissue retraction (Tomasek et al., 2002). During normal healing after tissue injury, these events allow wound contraction and resolution to occur. However, in the context of CKD and other fibrotic diseases, persistent myofibroblast activity, driven by TGFB1, results in pathological development of fibrosis.

TGFB1 is able to signal through serine-threonine kinase transmembrane receptors (type I and type II receptor heterodimers), which directly phosphorylate the downstream intracellular receptor-regulated SMAD proteins (R-SMADs) SMAD2 and SMAD3 (Shi and Massagué, 2003). R-SMAD heterocomplexes, along with SMAD4, are then translocated to the nucleus in order to regulate transcription of fibrotic genes such as α-SMA and collagens, by recruitment of transcriptional co-activators (Inoue et al., 2007). This pathway can be suppressed by ubiquitin-mediated destruction of TGFB receptors and R-SMADs, including SMAD7 (Fukuchi et al., 2001; Kavsak et al., 2000; Yan et al., 2016). Recent data show that SMAD ubiquitylation is reversible (Inui et al., 2011; Nan et al., 2016). Several studies have shown that TGFB1–SMAD3 signalling is required for renal fibrosis in mouse models of CKD (Fujimoto et al., 2003; Inazaki et al., 2004; Liu et al., 2012; Sato et al., 2003; Wang et al., 2007), raising the possibility of targeting this pathway to treat CKD.

SET9 (also known as SETD7) belongs to the evolutionarily conserved Su(var) enhancer of zeste and trithorax domain family containing lysine methyltransferases that are important in transcriptional regulation, and was originally shown to methylate lysine 4 in isolated histone H3 (H3K4) (Wang et al., 2001). Interestingly, however, SET9 only weakly methylates H3K4 in intact nucleosomes, and cells from the SET9-knockout mouse contain unaltered total methyl H3K4 levels (Lehnertz et al., 2011) pointing towards functional redundancy between methyltransferases and hinting at a role for SET9 elsewhere. SET9 was subsequently shown to regulate various transcription factors involved in differentiation, including p53, AR, ERα, NFκB, DNMT1, MyoD, FoxO3 and TAF10 (Calnan et al., 2012; Chuikov et al., 2004; Ea and Baltimore, 2009; Esteve et al., 2009; Gaughan et al., 2011; Kouskouti et al., 2004; Subramanian et al., 2008; Tao et al., 2011) and non-transcriptional proteins (Oudhoff et al., 2016; Shan et al., 2013). Nevertheless, because SET9 appears to be dispensable for p53 function *in vivo* and SET9-deficient mice undergo normal development (Campaner et al., 2011; Lehnertz et al., 2011) questions have again been raised over the true role of this methyltransferase (Keating and El-Osta, 2013).

Recent work has demonstrated that SET9 is involved in TGFB1-mediated ECM production in pulmonary fibrosis by a mechanism involving direct lysine methylation, and ubiquitin-mediated degradation of SMAD7 (Elkouris et al., 2016). Complementary work has shown that SET9 regulates ECM gene expression at a more downstream transcriptional level, through histone H3 monomethylation (Sun et al., 2010) and that SET9 inhibition may reduce fibrosis in a mouse model of ureteric obstruction (Sasaki

[1]Institute of Cellular Medicine, The Medical School, Framlington Place, Newcastle University, Newcastle upon Tyne, NE2 4HH, UK. [2]Northern Institute for Cancer Research, Paul O'Gorman Building, Framlington Place, Newcastle University, Newcastle upon Tyne, NE2 4HH, UK. [3]Dept of Chemistry, Biophysical Sciences Institute, Durham University, South Road, Durham, DH1 3LE, UK.
*These authors contributed equally to this work

‡Author for correspondence (i.r.logan@ncl.ac.uk)

I.R.L., 0000-0002-2838-0063

Received 25 June 2017; Accepted 27 November 2017

et al., 2016). Whilst these studies define an important role for SET9 in ECM production, the role of SET9 in governing key fibroblast activities, including myofibroblast differentiation, wound healing and collagen contractility, remains unexplored. Additionally, the possibility that SET9 regulates R-SMADs also remains unexplored.

Here, we demonstrate a novel interaction between SET9 and SMAD3, the key downstream R-SMAD in the TGFB1 pathway that is required for renal fibrosis. We show that SET9 regulates SMAD3 through multiple molecular mechanisms and influences important TGFB1-mediated processes including collagen contractility and α-SMA-driven differentiation of primary human kidney fibroblasts. We propose that pharmacological inhibition of SET9 could be important in the treatment of CKD.

RESULTS

SET9 is required for the fibroblast response to TGFB1

Given the uncertainty over SET9 function, we examined global gene expression in *Set9*$^{-/-}$ mouse embryonic fibroblasts (MEFs) compared with MEFs from wild-type (*Set9*$^{+/+}$) mice. Under normal growth conditions we observed that 760 genes were expressed at 1.5-fold or higher (range, 1.5- to 67-fold) in *Set9*$^{+/+}$ compared with *Set9*$^{-/-}$ MEFs (Table S2). Gene set enrichment analysis (GSEA) of these 760 genes produced cytoskeleton, wound healing and extracellular matrix amongst the 6 highest-ranked annotations – processes that are known to be regulated by TGFB1 (Table 1). We additionally treated MEFs with TGFB1 for 48 h. Under these conditions the number of differentially expressed genes in *Set9*$^{+/+}$ compared with *Set9*$^{-/-}$ MEFs increased to 2434 (range 1.5- to 66.53-fold, Table S3). Of the 760 genes differentially expressed under normal growth conditions 644 genes were also found to be differentially expressed among the 2343 genes altered upon TGFB1 treatment, demonstrating consistent effects of loss of SET9. GSEA of the 2343 SET9-regulated genes increased gene numbers under the previously listed annotations, in particular cytoskeleton, ubiquitin conjugation and extracellular matrix (Table 1). Additional data from a 24 h TGFB1 time point indicated that the highest ranking annotations remain enriched in response to TGFB1 treatment, including extracellular matrix, ubiquitin conjugation (the highest two ranking of all annotations at 24 h TGFB1 treatment) and cytoskeleton (Tables S1,S4). Overall, we conclude that SET9 is required for the fibroblast response to TGFB1.

SET9 interacts with and is a co-activator for SMAD3

We next examined whether SET9 could regulate TGFB1 signalling through downstream signalling mechanisms. We studied SMAD3, the principal factor that propagates TGFB1 signalling to the nucleus, in HKC-8 cells that are known to have an intact TGFB1 pathway. Immunoprecipitation of endogenous SET9 resulted in co-immunoprecipitation of SMAD3, in contrast to immunoprecipitation with control immunoglobulins (Fig. 1A). We observed enrichment of the SMAD3–SET9 interaction upon exogenous TGFB1 treatment. In a reciprocal experiment, immunoprecipitation of endogenous SMAD3 resulted in co-immunoprecipitation of SET9 (Fig. S1A). Even upon adjustment of cell lysates to 600 mM sodium chloride, we could still co-immunoprecipitate SET9 in a specific manner (Fig. S1A), demonstrating a strong SMAD3–SET9 interaction.

To exclude the possibility that antisera cross-reactivity caused these results, we immunoprecipitated overexpressed FLAG-tagged SET9 via the FLAG epitope. This resulted in co-immunoprecipitation of endogenous SMAD3, again with enrichment upon TGFB1 treatment (Fig. 1B). We next tested the SET9–SMAD3 interaction *in vitro*, free of other factors such as SMAD7, which might mediate indirect interactions. Immunoprecipitation with SMAD3 antibody led to co-immunoprecipitation of purified recombinant full-length SET9, only in the presence of SMAD3 (Fig. 1C). Conversely, immunoprecipitation of purified full-length SET9 led to co-immunoprecipitation of an N-terminal SMAD3 fragment (residues 1–211), containing the conserved MH1 domain, but not a C-terminal SMAD3 fragment (residues 199–425) (Fig. S1B). Control immunoglobulins did not immunoprecipitate significant quantities of any protein. Finally, we examined whether SET9 could interact with the transcriptionally active form of SMAD3, phosphorylated at C-terminal serine residues 423 and 425. Immunoprecipitation with a different SET9 antibody to that used in Fig. 1A resulted in co-immunoprecipitation of phosphorylated SMAD3 (Fig. S1C). We conclude for the first time that SET9 interacts directly with SMAD3, in a manner that is enhanced by TGFB1.

Given its role in transcriptional regulation, we examined the effects of SET9 upon SMAD3 activity, using reporter gene assays. SET9 overexpression resulted in a significant enhancement of luciferase expression driven by a synthetic promoter containing 12 basal SMAD3 CAGA binding sites (CAGA-luc), in a dose-dependent fashion (Fig. 2A). Conversely, introduction of a SET9 mutant (H297A) lacking methyltransferase activity suppressed reporter activity, in a dominant-negative manner. We also reduced SET9 levels by means of siRNA knockdown. This resulted in a significant reduction in CAGA-luc activity, even upon exogenous TGFB1 treatment (Fig. 2B). Finally, introduction of the characterised SET9 inhibitor R-PFI-2 also resulted in a significant reduction in CAGA-luc activity, suggesting that SET9 methyltransferase activity is required, at least in part, for the effects upon SMAD3 (Fig. 2C).

We also examined the effects of SET9 on a natural PAI1 *cis* element driving luciferase reporter gene expression, arguably of more physiological relevance and known to be responsive to SMAD3. Overexpression of SET9 again significantly increased reporter gene expression, whereas addition of SET9 siRNA reduced reporter activity (Fig. S2). Overall, we conclude that SET9 is a SMAD3 co-activator.

Table 1. SET9 regulates TGFB1-mediated processes

Annotation	Normal growth			10 ng/ml TGFB1		
	No. of genes	Enrichment	*P*	No. of genes	Enrichment	*P*
Cytoskeleton	53	8.91	4.9E−8	135	27.25	3.8 E−11
Ubiquitin conjugation	73	3.7	1.6E−10	206	4.63	5.0E−29
Wound healing and angiogenesis	22	3.29	8.8E−7	38	2.32	5.1E−6
Apoptosis	32	3.23	6.3E−5	56	3.62	8.7E−6
Metal ion binding	8	2.69	1.0E−3	9	1.33	6.6E−2
Extracellular matrix	24	2.33	9.5E−7	36	4.63	8.8E−4

Set9$^{-/-}$ and *Set9*$^{+/+}$ MEFs cultured under normal growth conditions or exposed to 10 ng/ml TGFB1 for 48 h were used for global gene expression analysis. Differentially expressed gene sets between *Set9*$^{-/-}$ and *Set9*$^{+/+}$ MEFs were used for GSEA (see Materials and Methods). The top six enriched annotations, ranked by fold enrichment over genes returned by chance from a random gene set of identical size are listed. *P*-values were calculated using Fisher's exact test.

Journal of Cell Science (2018) 131, jcs207761. doi:10.1242/jcs.207761

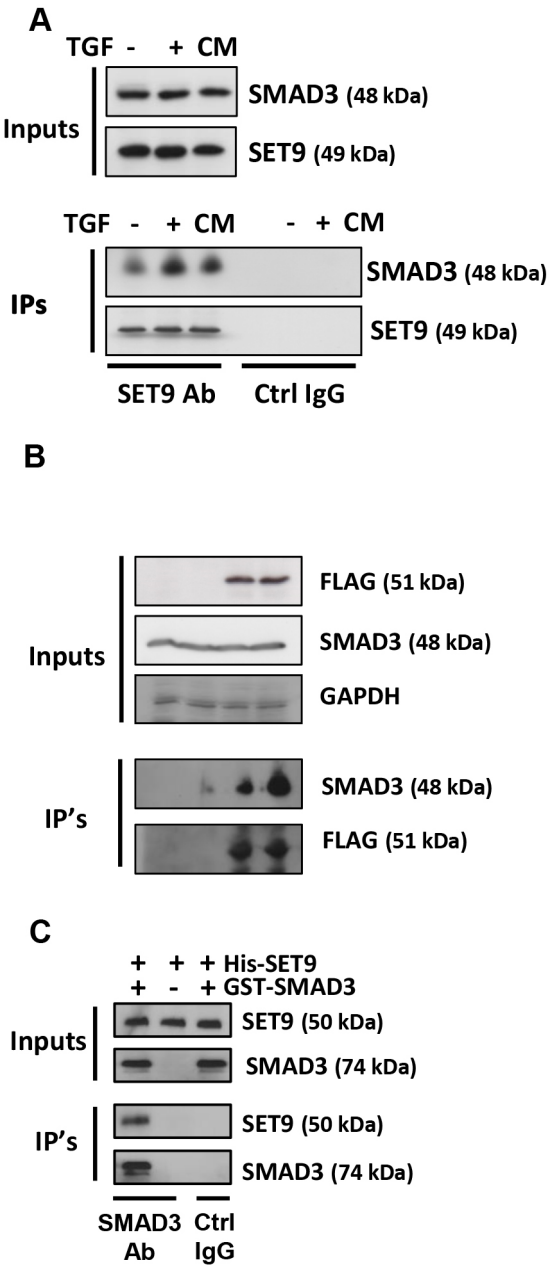

Fig. 1. SET9 interacts with SMAD3. (A) HK C-8 cells were cultured for 36 h in serum-free medium or complete medium (CM) then treated with DMSO vehicle (–) or 5 ng/ml TGFB1 (+) overnight. Immunoprecipitations (IPs) with either SET9 EPR5574 or control antibody (Ctrl IgG) were followed by immunoblotting as indicated. Representative experiments of three are shown. (B) HK C-8 cells were transfected with FLAG-SET9 or empty control vector overnight, starved for 24 h in serum-free medium prior to treatment with DMSO vehicle or 5 ng/ml TGFB1 overnight. Immunoprecipitation was then performed using FLAG antibody prior to immunoblotting as indicated. (C) Purified recombinant full-length SET9 and SMAD3 proteins were mixed in PBS prior to immunoprecipitation with SMAD3 Ab28379 antibody, extensive washes, then immunoblotting as shown.

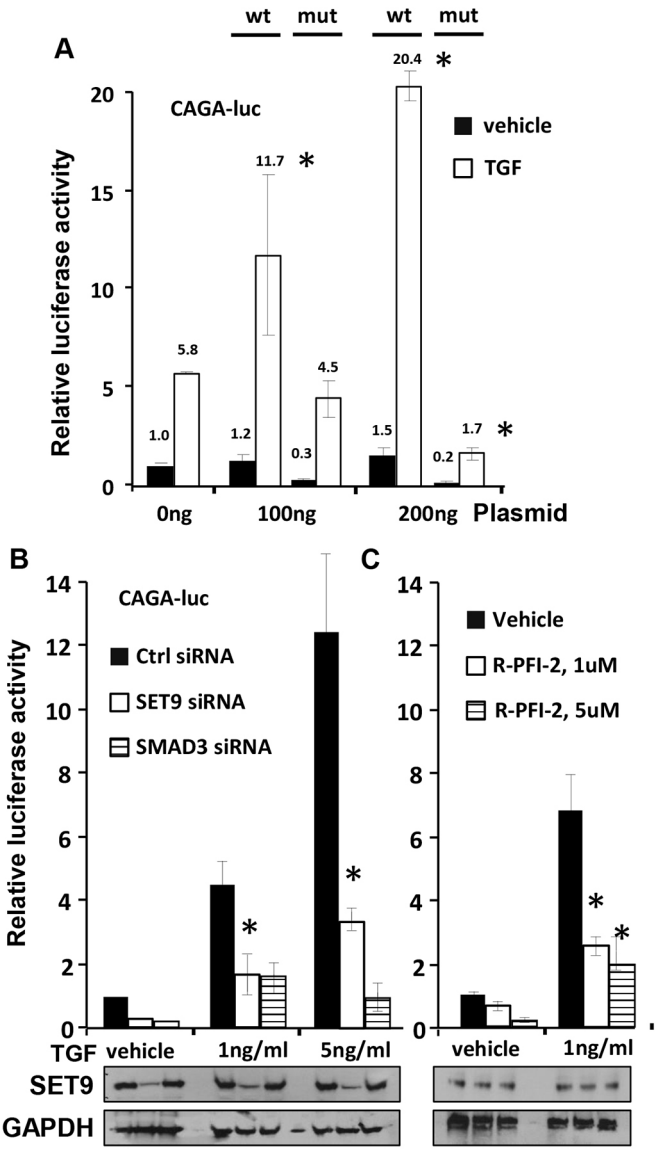

Fig. 2. SET9 is a SMAD3 co-activator. (A) HK C-8 cells transfected with 100 ng CAGA-luc and either 100 ng or 200 ng of plasmid encoding wild-type SET9 (wt) or H297A methyltransferase-deficient SET9 (mut); *n*=4. Empty vector was used to standardise total quantity of transfected DNA. Transfectants were starved in serum-free medium for 24 h then treated overnight with 5 ng/ml TGFB1 prior to luciferase assay. (B) HK C-8 cells transfected for 12 h with either control (Ctrl) siRNA or those targeting SET9 or SMAD3, then transfected the following day with CAGA-luc as above, starved in serum-free medium for 24 h, then treated overnight with TGFB1 where indicated, prior to luciferase assay. (C) HK C-8 cells transfected overnight with 100 ng CAGA-luc plasmid were starved in serum-free medium for 24 h containing DMSO vehicle or R-PFI-2, where indicated. Cells were then treated with TGFB1 overnight as shown, prior to luciferase assay. Lower panels in B and C show western blot results. Results are mean±s.d.; all results are representative of *n*=3 experiments. **P*<0.05 compared with respective control (*t*-test).

SMAD3 nuclear import and protein stability are dependent upon SET9

To further understand how SET9 controls SMAD3 activity, we examined the key regulatory steps in TGFB1 signalling: SMAD3 nuclear translocation and protein turnover. We firstly reduced SET9 levels by using siRNA, then assessed SMAD3 immunofluorescence. Compared with cells transfected with control siRNA, in which we observed principally nuclear staining for SMAD3, we noted a marked redistribution of SMAD3 to the cytoplasm upon knockdown of SET9 (Fig. 3A). Additionally, subcellular fractionation demonstrated that SMAD3 shifted from the cytoplasm in response to TGFB1, whereas SET9 siRNA that achieved a median 75% knockdown produced a persistent cytoplasmic pool of SMAD3 (Fig. 3B); in the absence of

Journal of Cell Science (2018) 131, jcs207761. doi:10.1242/jcs.207761

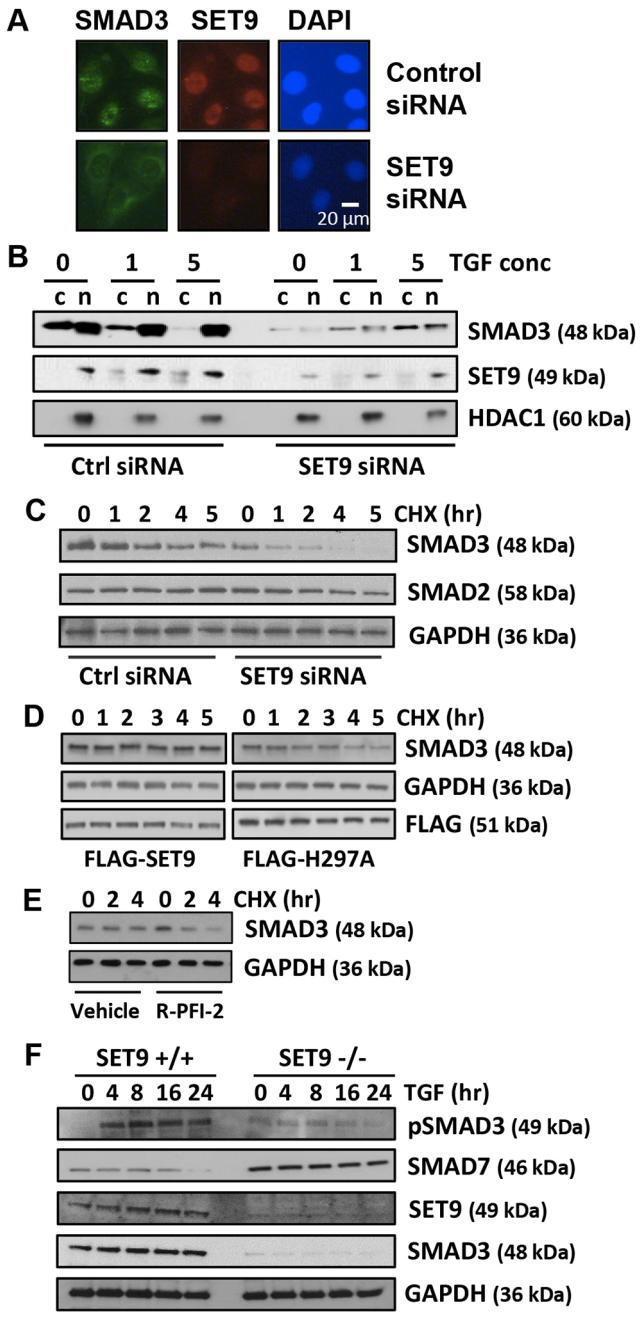

Fig. 3. SET9 regulates SMAD3 nuclear import and protein turnover. (A) HK C-8 cells were transfected with either control siRNA or those targeting SET9 for 12 h, starved in serum-free medium for 24 h prior to overnight treatment with 5 ng/ml TGFB1. Fixed cells were stained with the indicated antibodies and appropriate Alexa Fluor-labelled secondary antibodies. Control slides with control primary antisera did not exhibit fluorescence (not shown). (B) HK C-8 cells were transfected and starved as in A then treated with vehicle (0) or TGFB1 (1–5 ng/ml) overnight. Nuclear (n) and cytoplasmic (c) fractions were subject to immunoblotting as indicated, using HDAC1 as a nuclear marker. (C) HK C-8 cells were transfected and starved as in A then treated with TGFB1 (5 ng/ml) overnight. 50 µg/ml cycloheximide (CHX) was then applied for the indicated times prior to western blotting as indicated. (D) HK C-8 cells stably expressing wild-type FLAG-SET9 or methyltransferase-deficient FLAG-H297A mutant SET9 were treated as in C. (E) HK C-8 cells stably expressing wild-type FLAG-SET9 were treated as in C, except that 5 µM R-PFI-2 was added at the same time as TGFB1, prior to cycloheximide (CHX) application for the indicated times. (F) *Set9*$^{+/+}$ or *Set9*$^{-/-}$ MEFs were treated with 5 ng/ml TGFB1 for the indicated time points, prior to immunoblotting with the indicated antibodies. All results are representative of *n*=3 experiments (except for B, where *n*=2).

exogenous TGFB1, the percentage of total SMAD3 in the nucleus changed from 58% to 49% upon SET9 knockdown but in the presence of exogenous TGFB1, the percentage of total SMAD3 in the nucleus was reduced from 90% to 49% upon knockdown of SET9. We conclude that SET9 regulates TGFB1-driven nuclear import of SMAD3. We noted lower SMAD3 levels upon SET9 knockdown, which we investigated further.

To understand how SET9 alters SMAD3 levels, we firstly measured SMAD3 half-life, using cycloheximide (CHX) to block *de novo* protein synthesis. We observed a SMAD3 half-life of approximately 118 min in control cells (Fig. 3C). However, upon SET9 knockdown there was a lower steady state level of SMAD3, and increased SMAD3 turnover, with a half-life of approximately 48 min, which is less than half that of the control transfectants (Fig. 3C). No such effect could be seen upon SMAD2 (Fig. 3C). To exclude a confounding effect of transfection, we also examined SMAD3 half-life in *Set9*$^{-/-}$ MEFs. Compared with wild-type MEFs, SMAD3 was present at a similar steady state level (Fig. S3A), but exhibited a shorter half-life in *Set9*$^{-/-}$ cells upon CHX treatment (Fig. S3B). Finally, in order to understand whether or not SET9 methyltransferase activity was required to modulate SMAD3 turnover, we examined SMAD3 half-life in stably transfected cells expressing either wild-type or the H297A methyltransferase-deficient SET9. Cells expressing wild-type SET9 demonstrated entirely stable SMAD3 levels, whereas those expressing H297A mutant SET9 exhibited loss of SMAD3 upon CHX treatment (Fig. 3D). We could reverse the stabilising effect of wild-type SET9 upon SMAD3 by addition of the SET9 inhibitor R-PFI-2 (Fig. 3E). We conclude that SET9 stabilises SMAD3 in a methyltransferase-dependent manner.

We have observed a direct interaction between SET9 and SMAD3, and effects of SET9 upon SMAD3, whereas others have shown that SET9 regulates SMAD7. We therefore examined the effects of loss of SET9 upon SMAD7, in the *Set9*$^{-/-}$ MEF cells exposed to TGFB1. Compared with *Set9*$^{+/+}$ cells, the *Set9*$^{-/-}$ cells exhibited markedly increased levels of SMAD7, a failure to induce SMAD3 phosphorylation in response to exogenous TGFB1, and lower levels of total SMAD3 protein (Fig. 3F). These data confirm the important regulatory effect of SET9 upon SMAD7 levels described by Elkouris et al. (2016), but also suggest that SET9 directly influences SMAD3 levels.

To explore SMAD3 turnover in more detail we examined ubiquitylation, a process known to target SMAD3 for proteasomal destruction. We established a nickel agarose (Ni-NTA) pull-down assay to recover ubiquitylated SMAD3 by means of transfection of HIS-tagged ubiquitin. Addition of the proteasomal inhibitor MG-132 resulted in enrichment of high molecular weight SMAD3 species, characteristic of ubiquitylated SMAD3 (data not shown). Given the effects of SET9 methyltransferase activity on SMAD3 turnover, we incorporated the SET9 inhibitor R-PFI-2 (Barsyte-Lovejoy et al., 2014). Treatment of cells with low doses of MG-132 and R-PFI-2 resulted in an enrichment of ubiquitylated SMAD3 compared with that of cells treated with a low dose of MG-132 alone (Fig. 4A). We also examined ubiquitylation in cells stably expressing wild-type SET9 or methyltransferase-deficient H297A SET9. We observed a relative enrichment in ubiquitylated SMAD3 from cells expressing the H297A mutant in comparison to cells expressing wild-type SET9 (Fig. 4B). We conclude that SET9 methyltransferase activity is involved in regulating SMAD3 stability, in a manner that influences SMAD3 ubiquitylation and proteasomal destruction.

To test whether or not SET9 can directly methylate SMAD3, we used both recombinant full-length SMAD3 and a series of SMAD3

Journal of Cell Science (2018) 131, jcs207761. doi:10.1242/jcs.207761

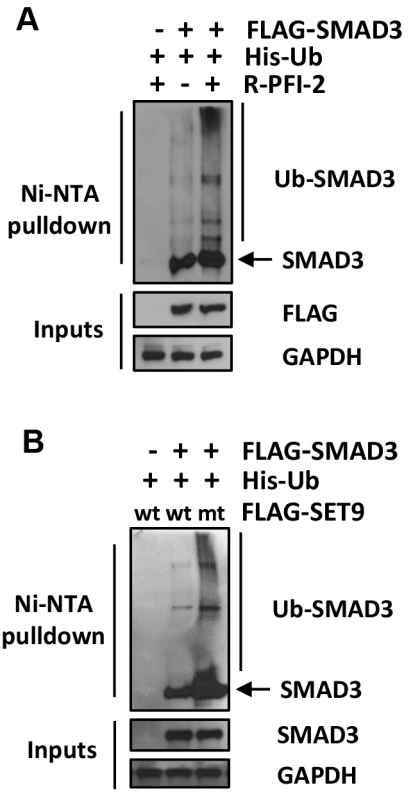

Fig. 4. SET9 regulates SMAD3 ubiquitylation. (A) HK C-8 cells were transfected with His-tagged ubiquitin (His-Ub) and either empty vector or FLAG-SMAD3 prior to treatment with 5 ng/ml TGFB1 for 24 h. Either DMSO vehicle or R-PFI-2 was then applied overnight along with 1 µM MG-132 prior to Ni-NTA pulldowns then immunoblotting. All cells received MG-132 and TGFB1. Ubiquitylated SMAD3 species are indicated (Ub-SMAD3). (B) HK C-8 cells stably expressing wild-type FLAG-SET9 (wt) or methyltransferase-deficient FLAG-H297A (mt) were transfected and treated with TGFB1 and MG-132 as in A, then subjected to Ni-NTA pulldowns and immunoblotting as indicated. Ubiquitylated SMAD3 species detected with SMAD3 antibody are indicated (Ub-SMAD3). All results are representative of *n*=3 experiments.

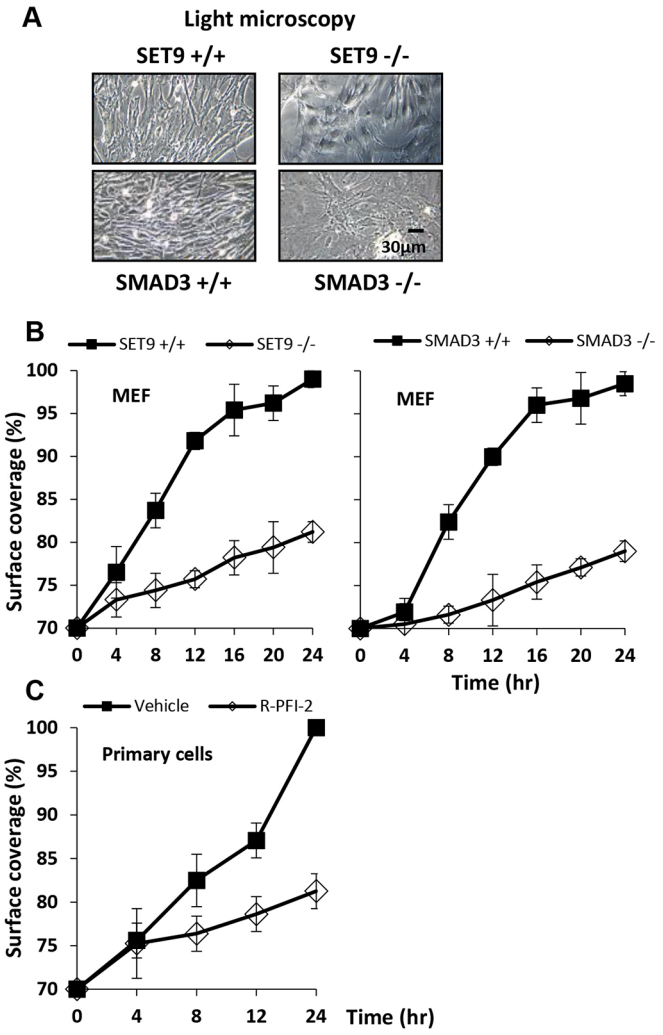

Fig. 5. SET9 regulates TGFB1-driven transformation and wound healing. (A) MEFs with the indicated genotypes were starved in 0.5% serum-containing medium for 36 h, then subject to overnight treatment with 5 ng/ml TGFB1 prior to light microscopy. (B) MEFs with the indicated genotypes were grown in cell culture inserts, in quadruplicate, overnight with 5 ng/ml TGFB1 or vehicle prior to wound formation by chamber removal. Wounds were photographed every 4 h, then surface coverage was calculated. (C) PRFs were treated as in B, except cells were simultaneously treated with either DMSO vehicle or 5 µM R-PFI-2 alongside 5 ng/ml TGFB1. Representative data from one patient of three are shown. Values are mean±s.d.

synthetic peptides as substrates for *in vitro* radioisotope-based methylation assays. Whilst we could readily detect methylation of histones by SET9, we failed to demonstrate methylation of either full-length SMAD3 or SMAD3 peptides. Additionally, we failed to detect methylation of the synthetic SMAD3 peptides by mass spectrometry (data not shown).

SET9 is involved in wound healing, contractility and ECM production in diseased renal fibroblasts

We evaluated the biological significance of SET9 in fibroblasts, which are known to be dependent upon TGFB1 and SMAD3 for differentiation to myofibroblasts (Evans et al., 2003). We again utilised MEFs, but also diseased human primary renal (myo)fibroblasts (PRFs) from fibrotic kidneys (three patients) and human mesangial cells. Whereas PRFs are responsible for tubulointerstitial fibrosis, mesangial cells cause glomerulosclerosis, the two entities constituting renal fibrosis in CKD.

Firstly, we examined fibroblast morphology. Whilst normal MEFs adopt a spindle-shaped appearance in response to TGFB1, in keeping with myofibroblast differentiation, *Set9*$^{-/-}$ MEFs failed to undergo this characteristic change (Fig. 5A), a phenotype also shared with *Smad3*$^{-/-}$ MEFs. Next, we examined fibroblast migration in wound healing assays in response to TGFB1, as a model of fibroblast recruitment in tissue injury. Whilst normal MEFs were capable of migrating to allow wound closure, *Set9*$^{-/-}$ MEFs were unable to do so (Fig. 5B), which is another property shared by *Smad3*$^{-/-}$ MEFs. Addition of the SET9 inhibitor R-PFI-2 to PRFs also significantly retarded the wound healing assay (Fig. 5C and Fig. S4A). This effect was reproducible in PRFs from all three patients (Fig. S4A). Normal MEFs and mesangial cells also exhibited equally poor wound closure upon R-PFI-2 treatment (data not shown). In the absence of TGFB1, R-PFI-2 had minimal effect on wound closure (Fig. S4B). We conclude for the first time that SET9 is important in fibroblast migration into the wound in response to TGFB1 – a key process in fibrosis.

We next assessed the role of SET9 in collagen contractility, an established methodology for studying myofibroblast–ECM interactions, and a model of tissue retraction in fibrosis (Grinnell, 2000). Compared with wild-type MEFs, *Set9*$^{-/-}$ MEFs exhibited significantly reduced collagen contractility (Fig. 6A), which was

Journal of Cell Science (2018) 131, jcs207761. doi:10.1242/jcs.207761

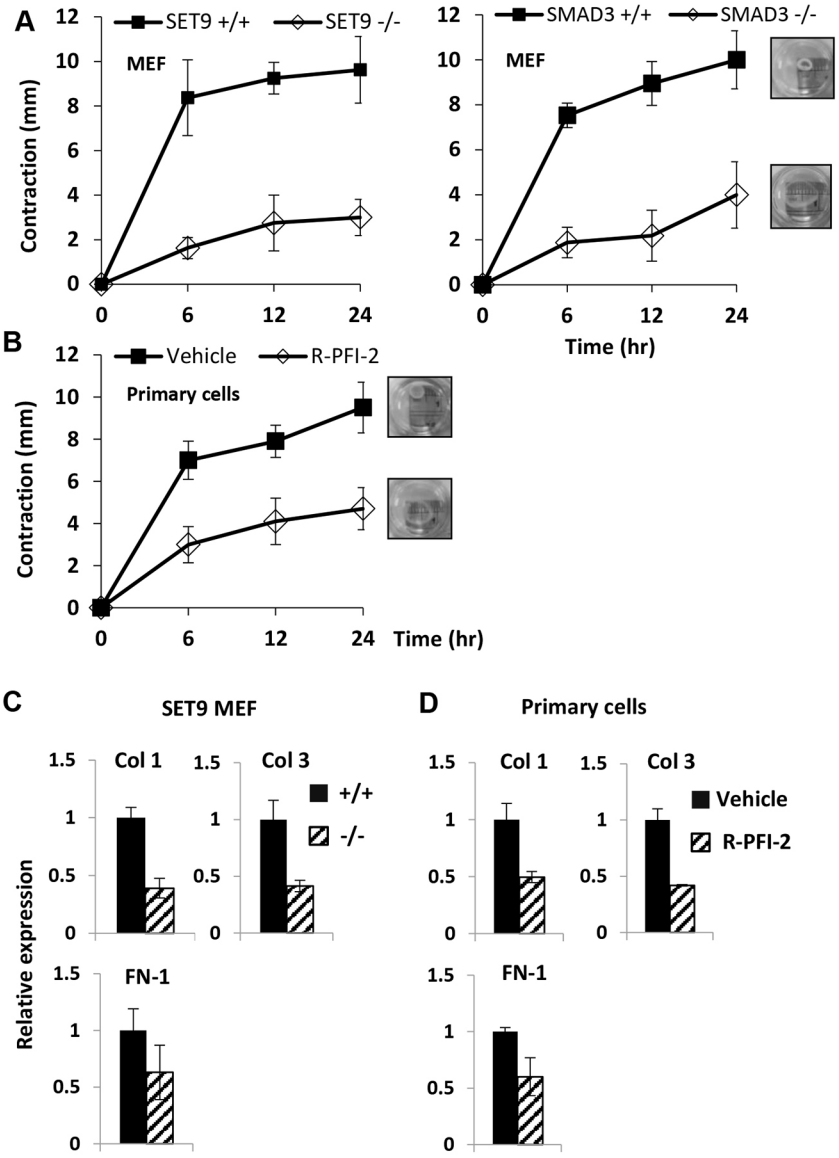

Fig. 6. SET9 regulates TGFB1-driven collagen contractility and fibrotic gene expression. (A) MEFs with the indicated genotypes were used in collagen contractility assays in triplicate, after treatment with 5 ng/ml TGFB1. Images show single representative collagen discs overlying ruler measure. (B) PRFs were treated as in A, except cells were simultaneously treated with either DMSO vehicle or 5 µM R-PFI-2 along with 5 ng/ml TGFB1. (C) MEFs with the indicated genotypes were seeded into glass chamber slides, starved in 0.5% serum-containing medium then treated with 5 ng/ml TGFB1 for 72 h prior to indirect immunofluorescence with the indicated antibodies. Four random images per slide were captured and ImageJ software used to determine relative levels of fluorescence. (D) PRFs from diseased kidneys were treated as in (C) except cells were treated with 5 ng/ml TGFB1 and either vehicle or 5 µM R-PFI-2 for 72 h prior to immunofluorescence. All results are representative of n=3 experiments; values are mean±s.d. All changes in C and D demonstrate statistical significance, P<0.05 (t-test).

phenotypically similar to *Smad3*$^{-/-}$ cells. This could be observed by measuring either collagen disc diameter or weight (Fig. 6A and data not shown). Addition of R-PFI-2 to PRFs from the three patients also showed a marked and reproducible reduction in collagen contractility (Fig. 6B). Application of R-PFI-2 to human mesangial cells or normal MEFs also resulted in a significant reduction in contractility (data not shown). In the absence of TGFB1, R-PFI-2 had minimal effect on collagen contractility (Fig. S4C). We infer that SET9 is required for fibroblast-mediated collagen contractility in response to TGFB1.

Next, we investigated the expression of ECM proteins. Previous studies have suggested that SET9 contributes to ECM production in lung fibrosis and mesangial cells (see Introduction) and collagens I and III are known to be key in fibrotic replacement of normal parenchyma. We observed significantly lower expression of collagens I and III and fibronectin-1 in *Set9*$^{-/-}$ MEFs versus wild-type MEFs in the presence of TGFB1 (Fig. 6C and Fig. S5A for example images). Importantly, treatment with R-PFI-2 significantly decreased the expression of ECM proteins in the diseased PRFs (Fig. 6C and Fig. S5B for example images). We deduce that SET9 is required for PRF expression of ECM in response to TGFB1, in keeping with previous reports (Elkouris et al., 2016; Sun et al., 2010).

SET9 regulates α-SMA expression and is recruited to the α-SMA gene promoter

Having shown altered myofibroblast contractility upon SET9 inhibition, we finally examined α-SMA, the most widely accepted marker of TGFB1-induced myofibroblast differentiation and contractility, but not previously known to be regulated by SET9. We established a chromatin immunoprecipitation assay to examine recruitment to the SMAD3 binding site within the α-SMA gene. Firstly, we observed a 2.6-fold enrichment of SMAD3, and a 3.8-fold enrichment of SET9, to the α-SMA gene but not the GAPDH gene, in response to TGFB1 in PRFs (Fig. 7A and Fig. S6A). These are the first data describing regulation of α-SMA by SET9. We then examined SET9 knockdown; we observed an ∼80% reduction in SMAD3 recruitment upon transfection of SET9 siRNA or SMAD3 siRNA (Fig. 7B and Fig. S6B). In keeping with a role for SET9 in SMAD3 protein turnover, the addition of MG-132 partly reversed the effect of SET9 knockdown on SMAD3 recruitment to the α-SMA gene. We went on to observe a ∼60% reduction in α-SMA

Journal of Cell Science (2018) 131, jcs207761. doi:10.1242/jcs.207761

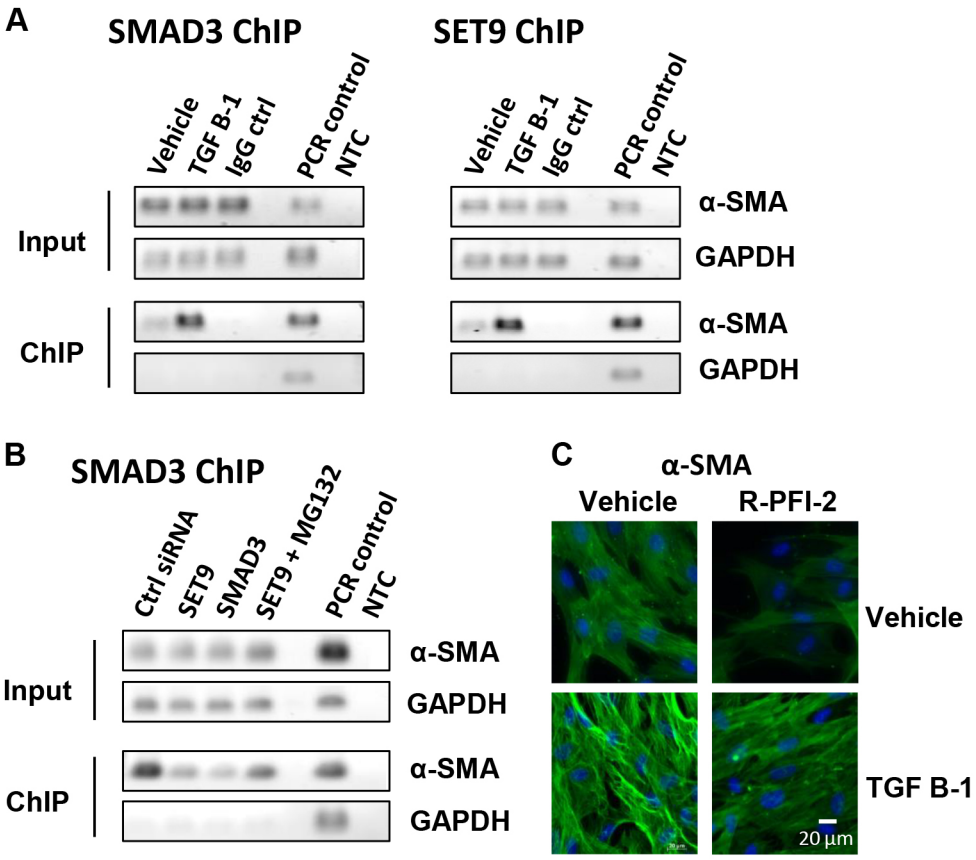

Fig. 7. SET9 regulates TGFB1-driven α-SMA expression. (A) PRFs were treated with either vehicle or 5 ng/ml TGFB1 for 24 h prior to chromatin immunoprecipitation with either SMAD3 Ab28379 (left) or SET9 C24B1 (right) antibodies. Control immunoglobulins (IgG ctrl) were included to show specificity. ChIP material was subject to PCR for either α-SMA or GAPDH to demonstrate selective recruitment. Purified human genomic DNA was used as a positive control in PCR (PCR control); NTC, no template control reaction. (B) PRFs were transfected with siRNA targeting either SET9, SMAD3 or control siRNA (Ctrl siRNA). 24 h later, all cells were treated with 5 ng/ml TGFB1 and 5 µM MG-132 where indicated. A further 24 h later, cells were used in chromatin immunoprecipitation assays with SMAD3 Ab28379, as described in A. (C) PRFs were treated simultaneously with either DMSO vehicle or 5 µM R-PFI-2 along with 5 ng/ml TGFB1 as in B and immunostained to detect α-SMA; nuclei are stained blue with DAPI. All results are representative of *n*=3 experiments; values are mean±s.d.

expression at the protein level in PRFs from all three patients in the presence of R-PFI-2, suggesting that SET9 inhibition prevents these cells from undergoing myofibroblast differentiation in response to TGFB1 (Fig. 7C). We also noted that addition of R-PFI-2 also reduced basal levels of α-SMA expression, which are likely to be stimulated by endogenous TGFB1 production. We conclude that SET9 is key to PRF differentiation and contractility in response to TGFB1.

DISCUSSION

Here, we show that SET9 interacts with SMAD3 and increases SMAD3 transcriptional activity, protein turnover and nuclear import. These are the first data showing this direct interaction and its effects on TGFB1 signalling.

Prior work has shown that the upstream regulatory protein SMAD7 is a target for SET9 methylation, resulting in its destruction through Arkadia-mediated ubiquitylation (Elkouris et al., 2016). SMAD3 protein levels, localization and transcriptional activity were not examined in that study. We confirm here that loss of SET9 stabilises SMAD7 in MEF cells. Interestingly, SMAD7 has recently been shown to interact with the conserved MH2 domain of SMAD3, resulting in SMAD3 destruction (Yan et al., 2016). Given that SET9 methylates SMAD7, it is possible that some of the effects of SET9 that we describe here are mediated, in part, through this indirect mechanism. For example, the stabilization of SMAD3 by SET9 we observed was dependent upon SET9 methyltransferase activity, but we could not demonstrate methylation of SMAD3 by SET9. This effect might therefore be indirectly mediated by SMAD7 methylation.

Nevertheless, we show that SET9 can interact directly with SMAD3 in the absence of SMAD7, and that SET9 interacts with the SMAD3 N-terminal MH1 domain, whereas SMAD7 was shown to interact with the C-terminal MH2 domain of SMAD3 (Yan et al., 2016). In keeping with SET9 having direct regulatory effects upon SMAD3, treatment of cells with the SET9 inhibitor R-PFI-2 or transfection of methyltransferase-deficient SET9 did not inhibit SMAD3 nuclear import (data not shown). If this effect was SMAD7 dependent, we predict that SET9 methyltransferase activity would be required. Additionally, the very low levels of total SMAD3 protein observed in *Set9*$^{-/-}$ cells suggest that SET9 has a direct influence on SMAD3 stability. We suggest that the different regulatory mechanisms upon SMADs – methylation and destruction in the case of SMAD7 but stabilization, nuclear import and transcriptional activation in the case of SMAD3 – makes SET9 a unique regulatory component of TGFB1 signalling. It is currently unclear whether SET9 interacts with other SMAD proteins aside from SMAD3 and SMAD7; however, we failed to identify an interaction between SMAD2 and SET9 by co-immunoprecipitation using antibodies against SMAD2 (data not shown).

Fibrosis is driven by TGFB1, which stimulates myofibroblast activities (Duffield, 2014). Whilst the origin of fibroblasts is debated, it is accepted that histologically confirmed fibrosis predicts poorer clinical outcomes in CKD (Menn-Josephy et al., 2016). There are no specific treatments to retard fibrosis (Tampe and Zeisberg, 2014). Previous work has shown that SET9 is important in ECM production in fibrosis (Elkouris et al., 2016; Sasaki et al., 2016) but the role of SET9 in other fibrotic processes is unclear. We demonstrate for the first time that SET9 is recruited to the α-SMA gene and that SET9 is required for SMAD3 occupancy at the α-SMA gene in PRFs, in response to TGFB1. These events coincide with TGFB1-mediated differentiation through expression of α-SMA, and increased collagen contractility. Taken together, our

data are consistent with a model in which SET9 mediates SMAD3 stabilization, nuclear import and subsequent recruitment to upregulate the α-SMA gene. Myofibroblast differentiation, α-SMA expression and collagen contractility are key features of fibrosis. Our results therefore suggest that SET9 inhibition might retard these myofibroblast activities in order to treat CKD (Duscher et al., 2014; Liu et al., 2003).

We additionally show for the first time that migration, which accounts for the presence of myofibroblast accumulation at the site of injury (Bochaton-Piallat et al., 2016), and perpetuation of fibrosis elsewhere within the organ, is dependent upon SET9. Previous work has shown that SET9 promotes ECM deposition in fibrosis; we also show that SET9 is required for ECM protein production, specifically in PRFs. Taken together, we propose that inhibition of myofibroblast accumulation at the site of injury, through targeting SET9, should reduce subsequent ECM deposition, as an additional means to treat CKD.

One limitation of our study is that it is currently unclear whether changes in gene expression, resulting from SET9 acting as a SMAD3 co-activator, account for all the phenotypic effects we observe in PRF cells. It is possible that some of the non-genomic effects of SET9 upon TGFB1–SMAD3 signalling we have observed might be responsible for the phenotypic effects of SET9 observed in myofibroblasts. We have not examined what proportion of genes altered in *Set9*$^{-/-}$ MEF cells in response to TGFB1 are co-regulated by SMAD3. It is possible that some of the gene expression changes we observe at the 48 h TGFB1 time point could result from activation of factors additional to SMAD3. Nevertheless, the stark differences in gene expression observed between the wild-type versus *Set9*$^{-/-}$ MEF cells, supports our original conclusion that SET9 is required for the global TGFB1 response, whether that is mediated solely through SMAD3 or via SMAD3 plus additional factors.

Recent data has suggested that loss of TGFB2 receptors does not prevent renal fibrosis in mouse models of CKD and that targeting upstream TGFB1 signalling in kidney disease may not be effective (Voelker et al., 2016). Nevertheless, SMAD3-deficient mice are resistant to renal fibrosis. Additionally, SMAD3 can be activated in a manner that is independent of TGFB1 to cause fibrosis (Chung et al., 2010; Li et al., 2004). It therefore remains likely that downstream signalling molecules such as SMAD3 and SET9 remain valid targets in CKD and other fibrotic diseases.

MATERIALS AND METHODS

Microarray and gene ontology

Set9$^{+/+}$ and *Set9*$^{-/-}$ MEFs were cultured in the presence or absence of TGFB1 before two-step total RNA extraction using Trizol and PureLink Micro scale columns (Life Technologies). RNA quality and cRNA synthesis was assessed and performed at The Wellcome Trust Centre for Human Genetics, as was cRNA hybridisation to Illumina Mouse WG-6 arrays. Quality control checks and normalisation was performed as described (Jones et al., 2015), again at that facility. Gene sets showing 1.5-fold or more upregulation between wild-type and *Set9*$^{-/-}$ MEFs were used for GSEA with the functional annotation tool of the DAVID Bioinformatics Resource v.6.8, default settings (Huang da et al., 2009a; Huang da et al., 2009b). The top six enriched annotations, ranked by fold enrichment over genes returned by chance from a random gene set of identical size are listed. Microarray data, including the full data gene sets can be found in Tables S2–S4.

Immunoprecipitation (IP), protein purification, antibodies

For IP, cells were lysed in 50 mM Tris-HCl, pH 7.4, 150 mM NaCl, 1 mM EDTA, 1% Triton X-100 with cOmplete protease inhibitors (Roche). Antibodies against SMAD3 (Abcam, Ab28379), SET9 (Millipore, EPR5574 or Cell Signaling Technology C24B1), FLAG (Sigma, F3165) or isotype control were crosslinked to Protein A Dynabeads using BS3 (Fisher). Where stated, lysates were adjusted to the required concentration of NaCl prior to immunoprecipitation with crosslinked antibodies overnight. For immunoblotting, SET9 rabbit monoclonal was used throughout (Cell Signaling Technologies, C24B1, 1:1000 dilution) and Veriblot secondary antibodies (Abcam, Ab131366, 1:1000 dilution) were used to avoid obscuring immunoglobulin chains. The two SMAD3 antibodies used, used at 1:1000 dilution, Ab28379 and phospho-SMAD3 423/425 (Cell Signaling Technology, C25A9) do not cross-react with other SMAD family members. Full-length recombinant SMAD3 (50991-M20B) and SET9 (14-469) were purchased from Sino Biologicals and Millipore, respectively. GST-tagged SMAD3 fragments were expressed from pGEX plasmids (Addgene) transformed into BL21 *E. coli* (Zhang et al., 1998) and purified over GST SpinTrap columns (GE Healthcare). Equimolar concentrations of recombinant proteins were mixed in PBS for 2 h prior to immunoprecipitation with the indicated antibodies, followed by extensive washing in PBS containing 0.05% Tween-20 and were then used for immunoblotting.

Fibroblast isolation, immunofluorescence, transfections, reporter assays and protein half-life analysis

Diseased renal fibroblasts from three patients were used in each assay described (DV Biologics). They were characterised by positive expression of vimentin, α-SMA, collagen I and III, electron microscopy and lack of tubular cell markers (not shown). For immunofluorescence, cells were seeded into glass chamber slides, treated as indicated, fixed with methanol and stained using antibodies listed (1:100 dilution). Fluorescence from Alexa Fluor-conjugated secondary antibodies (1:1000 dilution) was captured using a Zeiss Axioimager fluorescence microscope across four separate fields. Fluorescence in each field was then divided by the number of cells present (indicated by DAPI staining) to determine fluorescence per cell. Mean fluorescence across the four fields was then calculated and expressed as percentage of the highest values and subject to ANOVA statistical analysis. For western blot densitometry, ImageJ was used to subtract background signal from the band of interest prior to correction for signal arising from the relevant loading control.

Cells were transfected using Lipofectamine or RNAiMAX (Life Technologies) for plasmids or siRNA (30 nM), respectively. siRNA sequences have been described previously (Chuikov et al., 2004; Gaughan et al., 2011). Reporter assays were performed as described (Logan et al., 2009). Nuclear and cytoplasmic fractions were prepared using IGEPAL CA-630 (Sigma). For protein half-life assessment, cells transfected with siRNA or the indicated plasmids were treated with 50 µg/ml cycloheximide (Sigma) or DMSO vehicle for the indicated times prior to direct lysis into Laemmli buffer then immunoblotting. R-PFI-2 (Sigma) was used at the concentrations indicated.

Ubiquitylation, wound healing and collagen contractility analysis

To examine ubiquitylation, cells were transfected overnight with the indicated plasmids, treated with 10 ng/ml TGFB1 and low-dose 1 µM MG-132 then used for Ni-NTA chromatography as described (Logan et al., 2016). Wound healing assays were performed using two-chamber cell culture inserts (Ibidi). After allowing cells to adhere, they were treated as indicated then chambers removed and serial imaging performed to monitor wound closure, as stipulated by the manufacturer. For collagen contractility assays, 50,000 cells per sample were suspended into 0.5 ml of 0.65 mg/ml collagen I (BD Biosciences) in DMEM with 3.7 mM NaOH, per well of a 24-well plate then allowed to set for 30 min; 0.5 ml DMEM was then overlaid and matrices allowed to stress for 48 h. Matrices were then released from the well with a needle and serial diameter measurements taken. Sample weight was measured at the assay end point.

Chromatin immunoprecipitation

Chromatin from PRFs was prepared, after cross-linking cells in 1% formaldehyde for 10 min at room temperature, using ChromaFlash High-Sensitivity ChIP Kit (Epigentek); 20 µg chromatin was used, with 1 µg of the respective antibody. Oligonucleotide sequences 5′-TTTCAGCTTCC-CTGAACACC-3′ and 5′-CGGGTAATTAAAAGAGCCACTG-3′ were used to amplify the human sequence corresponding to the Rat SBE2

SMAD binding element, identified by sequence alignment (Hu et al., 2003), with 19 cycles of conventional PCR or SYBR green-based quantitative real-time PCR with ROX reference dye, incorporating melt curve analysis (Sigma S4438). GAPDH oligonucleotides were used as recommended in the ChIP kit.

Acknowledgements
We thank Guiseppe Testa for SET9 MEFs, Jill Norman for human mesangial cells, Peter ten Dijk for FLAG-SMAD3 and PAI1-luc, Caroline Hill for CAGA-luc, Erwin Bottinger for *Smad3*$^{-/-}$ cells and Adam Pickard for collagen contractility advice.

Competing interests
The authors declare no competing or financial interests.

Author contributions
Conceptualization: I.R.L., L.G., V.G.S., L.N., S.L.C., N.S.S.; Methodology: I.R.L., L.G., V.G.S., L.N., S.L.C., N.S.S.; Validation: I.R.L., N.S.S.; Formal analysis: I.R.L., L.N., N.S.S.; Investigation: I.R.L., L.G., V.G.S., L.N., C.A.M., S.L.C.; Resources: I.R.L., S.L.C., N.S.S.; Data curation: I.R.L., V.G.S.; Writing - original draft: I.R.L.; Writing - review & editing: I.R.L., L.G.; Visualization: N.S.S.; Supervision: I.R.L., N.S.S.; Project administration: I.R.L., N.S.S.; Funding acquisition: I.R.L., N.S.S.

Funding
We acknowledge Northern Counties Kidney Research Fund and the Academy of Medical Sciences for funding (I.L. and N.S.).

Supplementary information
Supplementary information available online at
http://jcs.biologists.org/lookup/doi/10.1242/jcs.207761.supplemental

References
Barsyte-Lovejoy, D., Li, F., Oudhoff, M. J., Tatlock, J. H., Dong, A., Zeng, H., Wu, H., Freeman, S. A., Schapira, M., Senisterra, G. A. et al. (2014). (R)-PFI-2 is a potent and selective inhibitor of SETD7 methyltransferase activity in cells. *Proc. Natl. Acad. Sci. USA* **111**, 12853-12858.

Bochaton-Piallat, M. L., Gabbiani, G. and Hinz, B. (2016). The myofibroblast in wound healing and fibrosis: answered and unanswered questions. *F1000Res* **5**, 752

Bottinger, E. P. and Bitzer, M. (2002). TGF-beta signaling in renal disease. *J. Am. Soc. Nephrol.* **13**, 2600-2610.

Calnan, D. R., Webb, A. E., White, J. L., Stowe, T. R., Goswami, T., Shi, X., Espejo, A., Bedford, M. T., Gozani, O., Gygi, S. P. et al. (2012). Methylation by Set9 modulates FoxO3 stability and transcriptional activity. *Aging (Albany NY)* **4**, 462-479.

Campaner, S., Spreafico, F., Burgold, T., Doni, M., Rosato, U., Amati, B. and Testa, G. (2011). The methyltransferase Set7/9 (Setd7) is dispensable for the p53-mediated DNA damage response in vivo. *Mol. Cell* **43**, 681-688.

Chuikov, S., Kurash, J. K., Wilson, J. R., Xiao, B., Justin, N., Ivanov, G. S., McKinney, K., Tempst, P., Prives, C., Gamblin, S. J. et al. (2004). Regulation of p53 activity through lysine methylation. *Nature* **432**, 353-360.

Chung, A. C. K., Zhang, H., Kong, Y. Z., Tan, J.-J., Huang, X. R., Kopp, J. B. and Lan, H. Y. (2010). Advanced glycation end-products induce tubular CTGF via TGF-beta-independent Smad3 signaling. *J. Am. Soc. Nephrol.* **21**, 249-260.

Duffield, J. S. (2014). Cellular and molecular mechanisms in kidney fibrosis. *J. Clin. Invest.* **124**, 2299-2306.

Duscher, D., Maan, Z. N., Wong, V. W., Rennert, R. C., Januszyk, M., Rodrigues, M., Hu, M., Whitmore, A. J., Whittam, A. J., Longaker, M. T. et al. (2014). Mechanotransduction and fibrosis. *J. Biomech.* **47**, 1997-2005.

Ea, C.-K. and Baltimore, D. (2009). Regulation of NF-kappaB activity through lysine monomethylation of p65. *Proc. Natl. Acad. Sci. USA* **106**, 18972-18977.

Elkouris, M., Kontaki, H., Stavropoulos, A., Antonoglou, A., Nikolaou, K. C., Samiotaki, M., Szantai, E., Saviolaki, D., Brown, P. J., Sideras, P. et al. (2016). SET9-mediated regulation of TGF-beta signaling links protein methylation to pulmonary fibrosis. *Cell Rep.* **15**, 2733-2744.

Esteve, P.-O., Chin, H. G., Benner, J., Feehery, G. R., Samaranayake, M., Horwitz, G. A., Jacobsen, S. E. and Pradhan, S. (2009). Regulation of DNMT1 stability through SET7-mediated lysine methylation in mammalian cells. *Proc. Natl. Acad. Sci. USA* **106**, 5076-5081.

Evans, R. A., Tian, Y. C., Steadman, R. and Phillips, A. O. (2003). TGF-beta1-mediated fibroblast-myofibroblast terminal differentiation-the role of Smad proteins. *Exp. Cell Res.* **282**, 90-100.

Fujimoto, M., Maezawa, Y., Yokote, K., Joh, K., Kobayashi, K., Kawamura, H., Nishimura, M., Roberts, A. B., Saito, Y. and Mori, S. (2003). Mice lacking Smad3 are protected against streptozotocin-induced diabetic glomerulopathy. *Biochem. Biophys. Res. Commun.* **305**, 1002-1007.

Fukuchi, M., Imamura, T., Chiba, T., Ebisawa, T., Kawabata, M., Tanaka, K. and Miyazono, K. (2001). Ligand-dependent degradation of Smad3 by a ubiquitin ligase complex of ROC1 and associated proteins. *Mol. Biol. Cell* **12**, 1431-1443.

Gaughan, L., Stockley, J., Wang, N., McCracken, S. R. C., Treumann, A., Armstrong, K., Shaheen, F., Watt, K., McEwan, I. J., Wang, C. et al. (2011). Regulation of the androgen receptor by SET9-mediated methylation. *Nucleic Acids Res.* **39**, 1266-1279.

Grinnell, F. (2000). Fibroblast-collagen-matrix contraction: growth-factor signalling and mechanical loading. *Trends Cell Biol.* **10**, 362-365.

Hinz, B., Celetta, G., Tomasek, J. J., Gabbiani, G. and Chaponnier, C. (2001). Alpha-smooth muscle actin expression upregulates fibroblast contractile activity. *Mol. Biol. Cell* **12**, 2730-2741.

Hu, B., Wu, Z. and Phan, S. H. (2003). Smad3 mediates transforming growth factor-beta-induced alpha-smooth muscle actin expression. *Am. J. Respir. Cell Mol. Biol.* **29**, 397-404.

Huang, D. W., Sherman, B. T. and Lempicki, R. A. (2009a). Bioinformatics enrichment tools: paths toward the comprehensive functional analysis of large gene lists. *Nucleic Acids Res.* **37**, 1-13.

Huang, D. W., Sherman, B. T. and Lempicki, R. A. (2009b). Systematic and integrative analysis of large gene lists using DAVID bioinformatics resources. *Nat. Protoc.* **4**, 44-57.

Inazaki, K., Kanamaru, Y., Kojima, Y., Sueyoshi, N., Okumura, K., Kaneko, K., Yamashiro, Y., Ogawa, H. and Nakao, A. (2004). Smad3 deficiency attenuates renal fibrosis, inflammation,and apoptosis after unilateral ureteral obstruction. *Kidney Int.* **66**, 597-604.

Inoue, Y., Itoh, Y., Abe, K., Okamoto, T., Daitoku, H., Fukamizu, A., Onozaki, K. and Hayashi, H. (2007). Smad3 is acetylated by p300/CBP to regulate its transactivation activity. *Oncogene* **26**, 500-508.

Inui, M., Manfrin, A., Mamidi, A., Martello, G., Morsut, L., Soligo, S., Enzo, E., Moro, S., Polo, S., Dupont, S. et al. (2011). USP15 is a deubiquitylating enzyme for receptor-activated SMADs. *Nat. Cell Biol.* **13**, 1368-1375.

Jones, D., Wade, M., Nakjang, S., Chaytor, L., Grey, J., Robson, C. N. and Gaughan, L. (2015). FOXA1 regulates androgen receptor variant activity in models of castrate-resistant prostate cancer. *Oncotarget* **6**, 29782-29794.

Kavsak, P., Rasmussen, R. K., Causing, C. G., Bonni, S., Zhu, H., Thomsen, G. H. and Wrana, J. L. (2000). Smad7 binds to Smurf2 to form an E3 ubiquitin ligase that targets the TGF beta receptor for degradation. *Mol. Cell* **6**, 1365-1375.

Keating, S. T. and El-Osta, A. (2013). Transcriptional regulation by the Set7 lysine methyltransferase. *Epigenetics* **8**, 361-372.

Kouskouti, A., Scheer, E., Staub, A., Tora, L. and Talianidis, I. (2004). Gene-specific modulation of TAF10 function by SET9-mediated methylation. *Mol. Cell* **14**, 175-182.

Lehnertz, B., Rogalski, J. C., Schulze, F. M., Yi, L., Lin, S., Kast, J. and Rossi, F. M. V. (2011). p53-dependent transcription and tumor suppression are not affected in Set7/9-deficient mice. *Mol. Cell* **43**, 673-680.

Li, J. H., Huang, X. R., Zhu, H. J., Oldfield, M., Cooper, M., Truong, L. D., Johnson, R. J. and Lan, H. Y. (2004). Advanced glycation end products activate Smad signaling via TGF-beta-dependent and independent mechanisms: implications for diabetic renal and vascular disease. *FASEB J.* **18**, 176-178.

Liu, X., Wen, F.-Q., Kobayashi, T., Abe, S., Fang, Q., Piek, E., Bottinger, E. P., Roberts, A. B. and Rennard, S. I. (2003). Smad3 mediates the TGF-beta-induced contraction of type I collagen gels by mouse embryo fibroblasts. *Cell Motil. Cytoskeleton* **54**, 248-253.

Liu, Z., Huang, X. R. and Lan, H. Y. (2012). Smad3 mediates ANG II-induced hypertensive kidney disease in mice. *Am. J. Physiol. Renal. Physiol.* **302**, F986-F997.

Logan, I. R., McNeill, H. V., Cook, S., Lu, X., Meek, D. W., Fuller-Pace, F. V., Lunec, J. and Robson, C. N. (2009). Heat shock factor-1 modulates p53 activity in the transcriptional response to DNA damage. *Nucleic Acids Res.* **37**, 2962-2973.

Logan, I. R., McClurg, U. L., Jones, D. L., O'Neill, D. J., Shaheen, F. S., Lunec, J., Gaughan, L. and Robson, C. N. (2016). Nutlin-3 inhibits androgen receptor-driven c-FLIP expression, resulting in apoptosis of prostate cancer cells. *Oncotarget* **7**, 74724-74733.

Massagué, J. (2012). TGFbeta signalling in context. *Nat. Rev. Mol. Cell Biol.* **13**, 616-630.

Menn-Josephy, H., Lee, C. S., Nolin, A., Christov, M., Rybin, D. V., Weinberg, J. M., Henderson, J., Bonegio, R. and Havasi, A. (2016). Renal interstitial fibrosis: an imperfect predictor of kidney disease progression in some patient cohorts. *Am. J. Nephrol.* **44**, 289-299.

Meran, S. and Steadman, R. (2011). Fibroblasts and myofibroblasts in renal fibrosis. *Int. J. Exp. Pathol.* **92**, 158-167.

Nan, L., Jacko, A. M., Tan, J., Wang, D., Zhao, J., Kass, D. J., Ma, H. and Zhao, Y. (2016). Ubiquitin carboxyl-terminal hydrolase-L5 promotes TGFbeta-1 signaling by de-ubiquitinating and stabilizing Smad2/Smad3 in pulmonary fibrosis. *Sci. Rep.* **6**, 33116.

Oudhoff, M. J., Braam, M. J. S., Freeman, S. A., Wong, D., Rattray, D. G., Wang, J., Antignano, F., Snyder, K., Refaeli, I., Hughes, M. R. et al. (2016). SETD7 controls intestinal regeneration and tumorigenesis by regulating Wnt/beta-Catenin and Hippo/YAP signaling. *Dev. Cell* **37**, 47-57.

Sasaki, K., Doi, S., Nakashima, A., Irifuku, T., Yamada, K., Kokoroishi, K., Ueno, T., Doi, T., Hida, E., Arihiro, K. et al. (2016). Inhibition of SET domain-containing lysine methyltransferase 7/9 ameliorates renal fibrosis. *J. Am. Soc. Nephrol.* **27**, 203-215.

Sato, M., Muragaki, Y., Saika, S., Roberts, A. B. and Ooshima, A. (2003). Targeted disruption of TGF-beta1/Smad3 signaling protects against renal tubulointerstitial fibrosis induced by unilateral ureteral obstruction. *J. Clin. Invest.* **112**, 1486-1494.

Shan, Z., Han, Q., Nie, J., Cao, X., Chen, Z., Yin, S., Gao, Y., Lin, F., Zhou, X., Xu, K. et al. (2013). Negative regulation of interferon-induced transmembrane protein 3 by SET7-mediated lysine monomethylation. *J. Biol. Chem.* **288**, 35093-35103.

Shi, Y. and Massagué, J. (2003). Mechanisms of TGF-beta signaling from cell membrane to the nucleus. *Cell* **113**, 685-700.

Subramanian, K., Jia, D., Kapoor-Vazirani, P., Powell, D. R., Collins, R. E., Sharma, D., Peng, J., Cheng, X. and Vertino, P. M. (2008). Regulation of estrogen receptor alpha by the SET7 lysine methyltransferase. *Mol. Cell* **30**, 336-347.

Sun, G., Reddy, M. A., Yuan, H., Lanting, L., Kato, M. and Natarajan, R. (2010). Epigenetic histone methylation modulates fibrotic gene expression. *J. Am. Soc. Nephrol.* **21**, 2069-2080.

Tampe, D. and Zeisberg, M. (2014). Potential approaches to reverse or repair renal fibrosis. *Nat. Rev. Nephrol.* **10**, 226-237.

Tao, Y., Neppl, R. L., Huang, Z.-P., Chen, J., Tang, R.-H., Cao, R., Zhang, Y., Jin, S.-W. and Wang, D.-Z. (2011). The histone methyltransferase Set7/9 promotes myoblast differentiation and myofibril assembly. *J. Cell Biol.* **194**, 551-565.

Tomasek, J. J., Gabbiani, G., Hinz, B., Chaponnier, C. and Brown, R. A. (2002). Myofibroblasts and mechano-regulation of connective tissue remodelling. *Nat. Rev. Mol. Cell Biol.* **3**, 349-363.

Voelker, J., Berg, P. H., Sheetz, M., Duffin, K., Shen, T., Moser, B., Greene, T., Blumenthal, S. S., Rychlik, I., Yagil, Y. et al. (2016). Anti-TGF-beta1 antibody therapy in patients with diabetic nephropathy. *J. Am. Soc. Nephrol.* **28**, 953-962.

Wang, H., Cao, R., Xia, L., Erdjument-Bromage, H., Borchers, C., Tempst, P. and Zhang, Y. (2001). Purification and functional characterization of a histone H3-lysine 4-specific methyltransferase. *Mol. Cell* **8**, 1207-1217.

Wang, A., Ziyadeh, F. N., Lee, E. Y., Pyagay, P. E., Sung, S. H., Sheardown, S. A., Laping, N. J. and Chen, S. (2007). Interference with TGF-beta signaling by Smad3-knockout in mice limits diabetic glomerulosclerosis without affecting albuminuria. *Am. J. Physiol. Renal. Physiol.* **293**, F1657-F1665.

Wynn, T. A. and Ramalingam, T. R. (2012). Mechanisms of fibrosis: therapeutic translation for fibrotic disease. *Nat. Med.* **18**, 1028-1040.

Yan, X., Liao, H., Cheng, M., Shi, X., Lin, X., Feng, X.-H. and Chen, Y.-G. (2016). Smad7 protein Interacts with receptor-regulated Smads (R-Smads) to inhibit transforming growth factor-beta (TGF-beta)/smad signaling. *J. Biol. Chem.* **291**, 382-392.

Zeisberg, M. and Kalluri, R. (2013). Cellular mechanisms of tissue fibrosis. 1. Common and organ-specific mechanisms associated with tissue fibrosis. *Am. J. Physiol. Cell Physiol.* **304**, C216-C225.

Zhang, Y., Feng, X.-H. and Derynck, R. (1998). Smad3 and Smad4 cooperate with c-Jun/c-Fos to mediate TGF-beta-induced transcription. *Nature* **394**, 909-913.